Optik - International Journal for Light and Electron Optics 286 (2023) 171033

Contents lists available at ScienceDirect

Optik

journal homepage: www.elsevier.com/locate/ijleo

(Invited) Kink solutions of the complex cubic– quintic Ginzburg-Landau equation in the presence of intrapulse Raman scattering

Ivan M. Uzunov [a,b], Vassil M. Vassilev [b], Todor N. Arabadzhiev [a,*], Svetoslav G. Nikolov [b,c]

[a] Department of Applied Physics, Faculty of Applied Mathematics and Informatics, Technical University of Sofia, 8 Kl. Ohridski Blvd., Sofia 1000, Bulgaria
[b] Institute of Mechanics, Bulgarian Academy of Sciences, Acad. G. Bonchev Str., Bl. 4, 1113 Sofia, Bulgaria
[c] Department of Mechanics, University of Transport, Geo Milev Str., 158, 1574 Sofia, Bulgaria

ARTICLE INFO

Keywords:
Nonlinear fiber optics
Soliton transmission systems
Fiber lasers
Intrapulse Raman scattering
Complex cubic– quintic Ginzburg-Landau equation

ABSTRACT

We present a study of solutions of the complex cubic–quintic Ginzburg-Landau equation (CCQGLE) and CCQGLE perturbed with the term responsible for the intrapulse Raman scattering (IRS). In both cases, using the method of first-order autonomous sub-equations, novel exact kink and antikink solutions have been identified. These solutions are represented in explicit analytic form. The numerical investigation of the influence of the IRS on the shape, amplitude, and velocity of the right side of the observed "front" CCQGLE solution revealed a good correlation with the identical features predicted by the newly discovered exact kink solution.

1. Introduction

The main physical factors determining the propagation of optical pulses in fiber-optic communication systems [1–3] and the formation of ultrashort optical pulses in lasers (solid –state and fiber lasers) [4,5] are: loss, dispersion, self-phase modulation, spectral filtering, saturated net-loss, saturated gain, and self-amplitude modulation [6–8]. The basic mathematical model for the description of all these phenomena is the complex cubic–quintic Ginzburg-Landau equation (CCQGLE) [9] and the related concept of dissipative solitons [10].

Although in the beginning CCQGLE was considered a qualitative model for the description of the optical phenomena [11], it was found later on that such a model could be connected with the parameters of the experimental setups (the mode-locked fiber lasers [12, 13]). Due to the importance of this equation, a huge interest has been focused on its solutions and their stability [14–20]. New analytical [15,16] and numerical solutions like pulsating solutions: plain pulsating, creeping, and erupting (exploding) solutions [17, 18] have been identified. Exact and numerical solutions of CCQGLE have been reviewed in [9,14,19].

A lot of investigations have been devoted to the study of the influence of different high-order effects on the above solutions [6–8]. An important higher-order effect is the stimulated Raman self-scattering of femtosecond optical solitons, experimentally discovered in [21,22]. This effect is also called intrapulse stimulated Raman scattering or simply intrapulse Raman scattering (IRS) [6,7,23,24]. In this regime of stimulated Raman scattering, the spectrum of a high-power ultrashort laser pulse proves to be so broad that it covers the

* Corresponding author.
E-mail address: tna@tu-sofia.bg (T.N. Arabadzhiev).

https://doi.org/10.1016/j.ijleo.2023.171033
Received 26 February 2023; Received in revised form 22 March 2023; Accepted 31 May 2023
Available online 1 June 2023

band of Raman resonances of the medium. In this case, the Stokes spectral component of the field shifted by the frequency of molecular vibrations is contained within the pump pulse itself. The amplification of low-frequency Stokes components in the field of high-frequency anti-Stokes spectral components of the same soliton pulse results in a continuous shift of its spectrum known as soliton Raman self-frequency shift [6,7,21–24]. The influence of intrapulse Raman scattering on the different solutions of the CCGLE and CCQGLE has been actively studied ([25–27] and referenced therein). The kink solution represents an optical front that preserves its shape when propagating through optical fiber [28–31]. We note that the influence of intrapulse Raman scattering on the kink solutions has been studied earlier in [28–30].

The aim of this article is to explore the existence of a novel kink solution of CCQGLE and CCQGLE perturbed by the term responsible for the intrapulse Raman scattering (IRS). Using the approaches of Akhmediev and Afanasjev [15] and Uzunov and Georgiev [32], respectively, novel exact kink and antikink solutions of the corresponding Ginzburg-Landau equation have been identified by applying the method of first-order autonomous sub-equations, see Conte and Musette [19, pp. 373–406]. The *method of first-order autonomous sub-equations* [19] is a particular case of the method of differential constraints [33–36]. In the case of CCQGLE perturbed with the term responsible for the intrapulse Raman scattering (IRS) our study can be considered as an extension of the earlier study [32]. Using an ansatz of the general form of the traveling wave, the equation of the nonlinear Liénard – Van der Pol oscillator for the amplitude of the nonlinear wave has been derived. The corresponding phase function can be calculated through the amplitude function. In this study, novel analytical kink solutions of the equation of the nonlinear Liénard – Van der Pol oscillator and therefore to the CCQGLE perturbed with the term responsible for the IRS are derived.

Next, we study numerically the influence of the IRS on the front solutions of CCQGLE. Moreover, we explore whether is it possible to identify the exact kink solution found here in the process of front propagation described by the numerical solution of CCQGLE. A numerical investigation of the CCQGLE has been performed through the split-step Fourier method (SSFM). This method has been proposed and developed by Tappert [37–39]. The SSFM has been further developed for the needs of consideration of higher-order effects [40–44]. Our numerical investigation utilizes Agrawal's split-step Fourier method with two iterations [44,45]. Due to the periodic boundary condition of our numerical method, we deal with the propagation of a combination of obtained kink solution and its mirror image [29,31]. Our numerical way of analysis of kink propagation in the presence of IRS follows the approach of [29].

The paper is organized as follows: First, the basic equation, and description of the numerical method for its solution are shortly given in Section2. Reductions to the ordinary differential equations (ODEs) of the basic CCQGLE and CCQGLE with the term responsible for IRS are described in Section 3. The new kink and antikink analytical solutions are presented there as well. In Section 4 we present the results of a numerical study of the influence of the intrapulse Raman scattering on the front solutions of CCQGLE. Here, we also explore the possibility to identify the novel kink analytical solution in the process of front propagation described by the numerical solution of CCQGLE. Finally, we make our conclusions in Section 5.

2. Basic equation and its numerical calculation

The basic equation which will be analyzed is the CCQGLE perturbed with IRS [6–9]:

$$i\frac{\partial U}{\partial x}+\frac{1}{2}\frac{\partial^2 U}{\partial t^2}+|U|^2U=i\delta U+i\beta\frac{\partial^2 U}{\partial t^2}+i\varepsilon|U|^2U-\nu|U|^4U+i\mu|U|^4U+\gamma U\frac{\partial}{\partial t}\left(|U|^2\right) \tag{1}$$

where U is the normalized envelope of the electric field, x and. are the evolutional and moving time frame variables, δ is the linear loss-gain coefficient, β describes the spectral filtering, ε is the nonlinear gain or absorption coefficient, μ, is the higher-order correction term to the nonlinear amplification (absorption), which, if negative, accounts for the saturation of the nonlinear gain [9,15–18], ν is the higher order correction term to the nonlinear refractive index [13–15] (if negative, it corresponds to the saturation of the nonlinear refraction index [9,15–18]). In this equation, we have implied that the group-velocity dispersion is anomalous. The parameter γ takes into account the effect of the IRS in the simplest quasi – instantaneous description [7]. Such a description of the IRS is valid for pulses shorter than 1 ps but wide enough to contain many optical cycles (pulse width $\geq 100fs$) [7]. Eq. (1) assumes a frame of reference moving with the pulse. Eq. (1) (without the term related to the IRS) has been originally proposed as a qualitative model [11], but now, as has already been mentioned, it can be directly connected to the parameters of the experimental setups of the real mode-locked fiber lasers [12,13].

For the numerical solution of Eq. (1), we have used Agrawal's split-step Fourier method with two iterations [44,45]. This method has shown the best robustness in long-range IRS modeling, which has been validated using a direct comparison of numerical results with analytical results from soliton perturbation theory [45]. The numerical parameters for our calculations are as follows: the number of samples: 2^{16}, time resolution 0.00244, frequency resolution 0.00625, constant step-size with value 10^{-4}.

As a result of intensive investigations of CCQGLE, numerical in [9] and analytical in [20] some areas in the space of parameters $(\delta,\beta,\varepsilon,\nu,\mu)$ of Eq. (1) have been established $(\delta<0,\beta>0,\varepsilon>0,\nu<0,\mu<0)$, in which there exist stable localized solutions of CCQGLE [9,20]. In what follows we will choose the value of these parameters in these areas.

3. Reduction to ordinary differential equations and exact solutions

One of the widely used methods for obtaining particular exact solutions to a partial differential equation in an explicit analytic form is to reduce it to ordinary differential equations. This is usually achieved through a suitable *ansatz* as it is done in the cases regarded below. Once such a reduction is accomplished, a great number of methods are available for determining exact solutions to the so-

obtained system of ordinary differential equations. In what follows, for that purpose we shall use the so-called *method of first-order autonomous sub-equations* (see [19]). It should be noted that this method is a particular case of the *method of differential constraints* (see [33,34,35, Chapter 4,36], and references therein). This method requires that the regarded system of equations be enlarged by appending an additional first-order autonomous equation such that the over-determined system obtained in this way be compatible.

3.1. Kink-like solutions to Eq. (1) with $\gamma = 0$

In [15] (see also, [16] and [9, Chapter 13]), stationary solutions of Eq. (1) with $\gamma = 0$ are sought in the form:

$$U(x,\ t) = a(t)\exp\{id\ \ln[a(t)] - i\omega x\} \tag{2}$$

where d (*the chirp parameter*) and ω are real constants. After substituting Eq. (2) into Eq. (1) and separating real and imaginary parts, one obtains the following over-determined system of equations for the amplitude function $a(t)$, namely:

$$\omega a + \left(\frac{1}{2} + \beta d\right)a'' + \left(\beta d - \frac{d^2}{2}\right)\ \frac{a'2}{a} + a^3 + \nu a^5 = 0 \tag{3}$$

$$\delta a - \left(\frac{d}{2} - \beta\right)a'' - \left(\frac{d}{2} + \beta d^2\right)\ \frac{a'2}{a} + \varepsilon^3 a^3 + \mu a^5 = 0 \tag{4}$$

where the primes denote differentiation with respect to the variable t. The following assertion can be verified by direct computation. This system turned out to be compatible provided that the coefficients d, ω, ε, β, δ, μ and ν meet the compatibility conditions (10) obtained in [16]. Various such cases are found in [15] (see also, [16] and [9, Chapter 13]). Let us, however, check what would happen if we enlarge the system (3), (4) with a first-order autonomous sub-equation of the form:

$$a' + A_1 a + A_3 a^3 = 0 \tag{5}$$

where A_1 and A_3 are some real constants. In fact, this is a constant coefficient Bernoulli equation with $n = 3$. Then, one can easily verify by direct computation that under the conditions:

$$\begin{aligned}
&\delta = \frac{2\omega\left(d^2\beta + d - \beta\right)}{d^2 - 4d\beta - 1},\quad \varepsilon = \frac{3d + 2\left(d^2 - 2\right)\beta}{d^2 - 6d\beta - 2}\\
&\mu = \frac{\left(d^2 - 4d\beta - 1\right)\left(d^2\beta + 2d - 3\beta\right)}{2\omega\left(d^2 - 6d\beta - 2\right)^2},\qquad \nu = \frac{\left(d^2 - 8d\beta - 3\right)\left(d^2\beta - 4d\beta - 1\right)}{2\omega\left(d^2 - 6d\beta - 2\right)^2}\\
&A_1 = \pm\frac{\sqrt{2\omega}}{\sqrt{d^2 - 4d\beta - 1}},\quad A_3 = \pm\frac{\sqrt{d^2 - 4d\beta - 1}}{\sqrt{2\omega}\left(d^2 - 6d\beta - 2\right)},
\end{aligned} \tag{6}$$

the Eqs. (3) –(5) are compatible, and each solution of an equation of the form:

$$a' \pm \frac{\sqrt{2\omega}}{\sqrt{d^2 - 4d\beta - 1}}a \pm \frac{\sqrt{d^2 - 6d\beta - 1}}{\sqrt{2\omega}\left(d^2 - 6d\beta - 2\right)}a^3 = 0 \tag{7}$$

satisfies both Eqs. (3) and (4). In this way, we obtain new stationary solutions of the form (2) to Eq.(1) with $\gamma = 0$, which are given through the amplitude functions of the form:

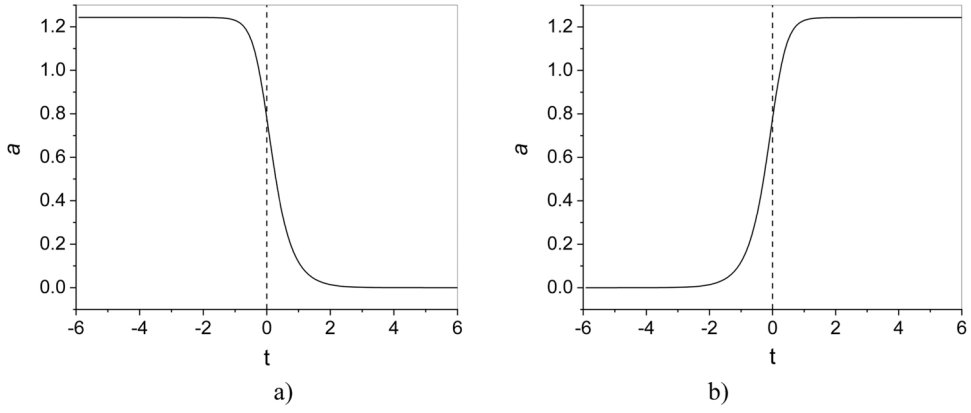

Fig. 1. Solutions of types a) kink and b) anti-kink of the form (8). Here, $C_1 = 1,\ t_0 = 0,\ d = 1,\ \omega = 1$ and $\beta = -0.11$.

$$a(t)=\frac{1}{\sqrt{\nu(t)}},\qquad \nu(t)=C_1\exp\left[\pm\frac{2\sqrt{2\omega}(t+t_0)}{\sqrt{d^2-4d\beta-1}}\right]-\frac{d^2-4d\beta-1}{2\omega\left(d^2-6d\beta-2\right)} \tag{8}$$

where C_1 and t_0 are arbitrary constants. These solutions, which turned out to be kink-like (see Fig. 1) are missed in [9,15,16].

In this case, kink and antikink solutions are mirror images of each other.

3.2. Kink-like solutions to Eq. (1) with $\gamma \neq 0$

In [32], it is shown that the complex partial differential Eq. (1) admits reduction to a system of ordinary differential equations through the ansatz:

$$U(x,t)=u(\xi)\exp(i(f(\xi)+Kx)) \tag{9}$$

where $\xi = t - Mx$, and M and K are real numbers. $u(\xi)$ and $f(\xi)$ are real-valued functions of the similarity variable ξ. Indeed, by substituting (9) into (1) and separating the real and imaginary parts of the obtained expression one obtains the following nonlinear system of ordinary differential equations for the amplitude and phase functions $u(\xi)$ and $f(\xi)$, namely:

$$\frac{1}{2}\,u''+2\beta\,u'\,f'-2\gamma u^2u'-Ku+\,Mu\,f'-(1/2)\,u\,(f')^2+\beta\,u\,f''+\,u^3+\nu u^5=0 \tag{10}$$

$$\beta u''-f'\,u'+Mu'+\delta u-\beta u(f')^2-(1/2)uf''+\varepsilon u^3+\mu u^5=0 \tag{11}$$

where the primes denote now differentiation with respect to the similarity variable ξ.

Using results presented in [32] for $\gamma \neq 0$, it can be verified by direct computation that under the condition:

$$v=\frac{\mu}{2\beta},\quad M=\frac{\left(1+4\beta^2\right)(\varepsilon-2\beta)}{4\beta^2\gamma}\;;\quad K=\frac{\left(1+4\beta^2\right)(\varepsilon-2\beta)^2}{16\beta^4\gamma^2}-\frac{\delta}{2\beta} \tag{12}$$

the differential constraint:

$$f'=\frac{M}{1+4\beta^2}+\frac{2\beta\gamma}{1+4\beta^2}u^2+\frac{c_0}{u^2}\exp\left(\frac{2\beta-\varepsilon}{\beta\gamma}\xi\right) \tag{13}$$

where c_0 is a real constant, is compatible with the system of Eqs. (10), (11) and leads to the single differential equation:

$$u''+\left(c_2+c_4u^2\right)u'+c_1u+c_3u^3+c_5u^5=c_0\exp\left(\frac{2\beta-\varepsilon}{\beta\gamma}\xi\right)\left[\frac{c_0}{u^3}\exp\left(\frac{2\beta-\varepsilon}{\beta\gamma}\xi\right)+\frac{4\beta\gamma}{1+4\beta^2}u\right] \tag{14}$$

for the amplitude function $u(\xi)$, where:

$$c_1=\frac{\delta}{\beta}-\frac{(\varepsilon-2\beta)^2}{16\beta^4\gamma^2},\;c_2=\frac{\varepsilon-2\beta}{\beta\gamma},c_3=\frac{2+4\beta\varepsilon}{1+4\beta^2},c_4=-\frac{4\gamma}{1+4\beta^2},c_5=\frac{\mu}{\beta}-\frac{4\beta^2\gamma^2}{\left(1+4\beta^2\right)^2} \tag{15}$$

In other words, each solution $(u\;,\;f)$ of the systems (13), (14) is a solution of the system (10), (11) as well provided that the conditions (12) hold. Eq. (13) implies the following expression for the phase function:

$$f=\frac{2\beta\gamma}{1+4\beta^2}\int u^2d\xi+\frac{M}{1+4\beta^2}\xi+f_0+c_0\int\frac{1}{u^2}\exp\left(\frac{2\beta-\varepsilon}{\beta\gamma}\xi\right)d\xi \tag{16}$$

wheref_0 is a real constant, and hence it is determined by quadratures once the amplitude function $u(\xi)$ is found. For that purpose, we have to solve Eq. (14). Hereafter, assuming $c_0 = 0$ we are going to analyze some possibilities for obtaining exact solutions of the respective equation of the form (14), i.e.:

$$u''+\left(c_2+c_4u^2\right)u'+c_1u+c_3u^3+c_5u^5=0 \tag{17}$$

Let us remark that Eq. (17) is of Liénard type [46]. The interested reader is referred to the recent papers [47,48] for a detailed analysis of the integrability and solvability of those types of equations.

In order to obtain particular solutions to Eq. (17) we will look for the conditions under which this equation is compatible with a sub-equation of the form:

$$u'+B_1u+B_3u^3=0, \tag{18}$$

where B_1 and B_3 are some real constants. This is again a constant coefficient Bernoulli equation with $n = 3$. Now, substituting the derivatives of the function u expressed via equation Eq. (18) into (17) one can easily verify by direct computation that under the conditions:

$$c_1 = \frac{9c_3^2 - 3c_2c_3\left(2c_4 \mp \sqrt{c_4^2 - 12c_5}\right) + 9c_2^2c_5}{48c_5 \pm 4c_4\sqrt{c_4^2 - 12c_5} - 5c_4^2} \tag{19}$$

$$B_1 = \frac{c_2\left(\sqrt{c_4^2 - 12c_5} \pm c_4\right) \mp 6c_3}{4c_4\sqrt{c_4^2 - 12c_5} \mp 2c_4} \quad , \quad B_3 = \frac{1}{6}\left(c_4 \pm \sqrt{c_4^2 - 12c_5}\right) \tag{20}$$

each solution of the respective Eq. (18) is a solution to Eq. (17) as well. Thus, we found kink-like solutions (see Fig. 2) of the form (9) to equations of the form (1), which are given through the following amplitude function:

$$u(\xi) = \frac{1}{\sqrt{v(\xi)}} \tag{21}$$

$$v(\xi) = \frac{c_4^2 \pm c_4\sqrt{c_4^2 - 12c_5} - 24c_5}{18c_3 - 3c_2\left(c_4 \pm \sqrt{c_4^2 - 12c_5}\right)} + C_2\exp\left[\frac{\left(c_2\sqrt{c_4^2 - 12c_5} \pm c_2c_4 \mp 6c_3\right)}{2\sqrt{c_4^2 - 12c_5} \mp c_4}(\xi + \xi_0)\right] \tag{22}$$

where C_2 and ξ_0 are arbitrary constants.

The presented in Fig. 2a exact kink solution given by Eq. (21) will be used in the next section as a part of the initial condition for numerical simulations. Note that the choice of values of parameters:$\delta = -0.0145769; \beta = 0.28; \varepsilon = 0.742; \nu = -0.482143; \mu = -0.2771; \gamma = 0.65$ satisfy earlier mentioned conditions [9,20] for observing stable solutions.

4. Numerical results

This section aims to present a numerical study of the influence of the intrapulse Raman scattering on the front solutions of CCQGLE. Moreover, we explore whether is it possible to identify the novel exact solution of Eq. (21) in the process of front propagation described by the numerical solution of CCQGLE. In what follows, we will have a special attitude to the described above example of kink (front) solutions predicted by Eq. (21).

According to [29,31] our initial condition will be formed as a construction (combination) of our exact kink solution and its mirror image. (This mirror image could be thought of as an "antikink" [29]). Such kind of formation (in some places we use common names for the formation - front or kink instead of fronts or kink and antikink) can be considered also as two fronts propagating from each other [31]. We could expect that the trailing part of the formation is related to the evolution of the exact kink solution. An important parameter in such a construction of the initial condition is a separation (spacing) between kink and antikink. This separation determines the initial time-width of our pulselike input and in our consideration, it has a magnitude of $2t_0$.

Before considering the influence of the IRS on the front propagation, however, we will present propagation of the front solution of CCQGLE with the parameters $\delta = -0.0145769, \beta = 0.28, \varepsilon = 0.742, \nu = -0.482143, \mu = -0.2771$ but in the condition of the absence of IRS i.e.$\gamma = 0$. Considering such a case is necessary to establish the influence of the IRS- see Fig. 3.

In Fig. 3a and Fig. 3b we clearly see, that after initial adjustment a stationary and stable front solution is formed. Precise conservation of the transverse profile of the solution is well observed in Fig. 3(b). (This result is similar to the ones of [31]). Note that the appearance of a sink plateau in the middle part of the front has been attributed to the chirp of continuous wave solution between kink and antikink [31]. The important influence of all nonlinear effects on the spectrum is illustrated in Fig. 3(c).

In the next Fig. 4 is presented the influence of IRS on the above front propagation. It should be mentioned that, as above, the value

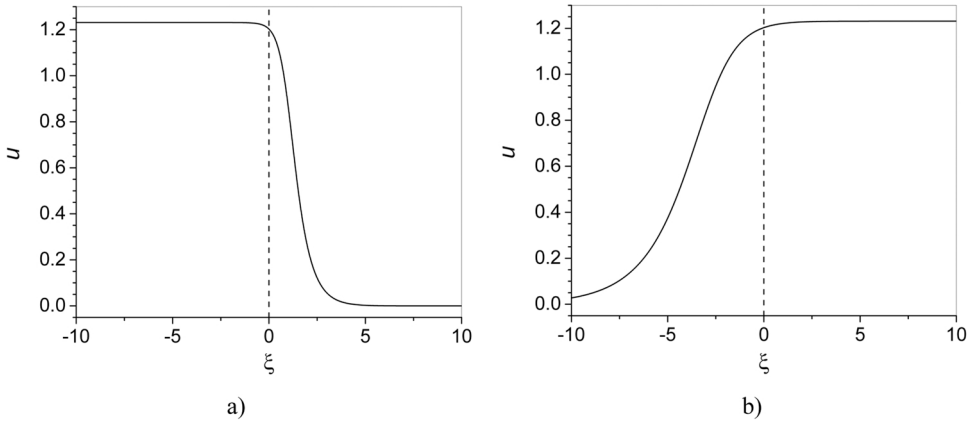

Fig. 2. Solutions of types: a) kink and b) anti-kink of the form (21). Here,$C_2 = 0.03143, \xi_0 = 0, M = 1.17286, K = 1.07322$. Parameters: $\delta = -0.0145769$, $\beta = 0.28$, $\varepsilon = 0.742$, $\nu = -0.482143, \mu = -0.2771, \gamma = 0.65$.

of the parameter describing the influence of IRS coincides with that predicted from our analytical solution.

It is seen in Fig. 4a and Fig. 4b that, as a result of the influence of IRS the stable front propagation in Fig. 3 is considerably disturbed. The temporal profile of the numerical solution during the front propagation is separated conditionally on the left and right parts. The left part, ("antikink") forms a stable shape and amplitude during its propagation, while the right part ("kink") after a short initial distance, recovers its original (initial) shape and amplitude, corresponding exactly to that presented in Fig. 2a exact kink solution of CCQGLE. The value of this amplitude is around 1.2 - the same as the value of our exact kink solution. Based on these observations we could connect the right part of our deformed front with the exact kink solution found in the previous section. Finally, in addition to the influence of all nonlinear effects on the spectrum, a transfer of energy to lower frequencies attributed to IRS can be observed (see Fig. 4c). In Fig. 4d, a time-shifted exact kink solution (so that it can be compared with the numerical solution) taken from Eq. (21) and part of the CCQGLE numerical solution taken around the right edge of the formation at $x = 20$ are presented. What we see in Fig. 4d is the good correlation between the obtained numerical results for the shape and amplitude of the right edge of the front and those characteristics of the predicted novel kink solution. Such correlation is observed after a short initial stage of evolution which leads to the appearance in the right part of the formation of a relatively stable kink, matching in shape, amplitude and velocity with the analytically represented by Eq. (21) kink solution. In the following figures - Fig. 5 and Fig. 6, we will also see that with different width and shape of the initial condition, this characteristic right part of the formation corresponding to the kink solution from Eq. (21) appears in each of the CCQGLE numerical solutions presented.

As has been mentioned above, an important parameter in the construction of the initial condition is a separation (spacing) between kink and antikink, which determines the initial width of our pulselike input. Below, Fig. 5 shows our numerical results for two additional values of t_0, namely 1 and 20.

As can be seen in Fig. 5 the change of initial separation (spacing) between kink and antikink (in that interval) does not result in the qualitative change from the observed behavior in Fig. 4. Moreover, we could see that the amplitudes of the right and left parts of our propagating front remain the same with the right-hand edge (the kink) always keeping its initial parameters corresponding to the exact solution of the CCQGLE.

In the expression of the similarity variable $\xi = t - Mx$, the real number. describes the "velocity" with which the kink and antikink move in time t during the propagation distance x. It is seen that in Fig. 3 (for $\gamma = 0$) the velocities of the two fronts propagating from

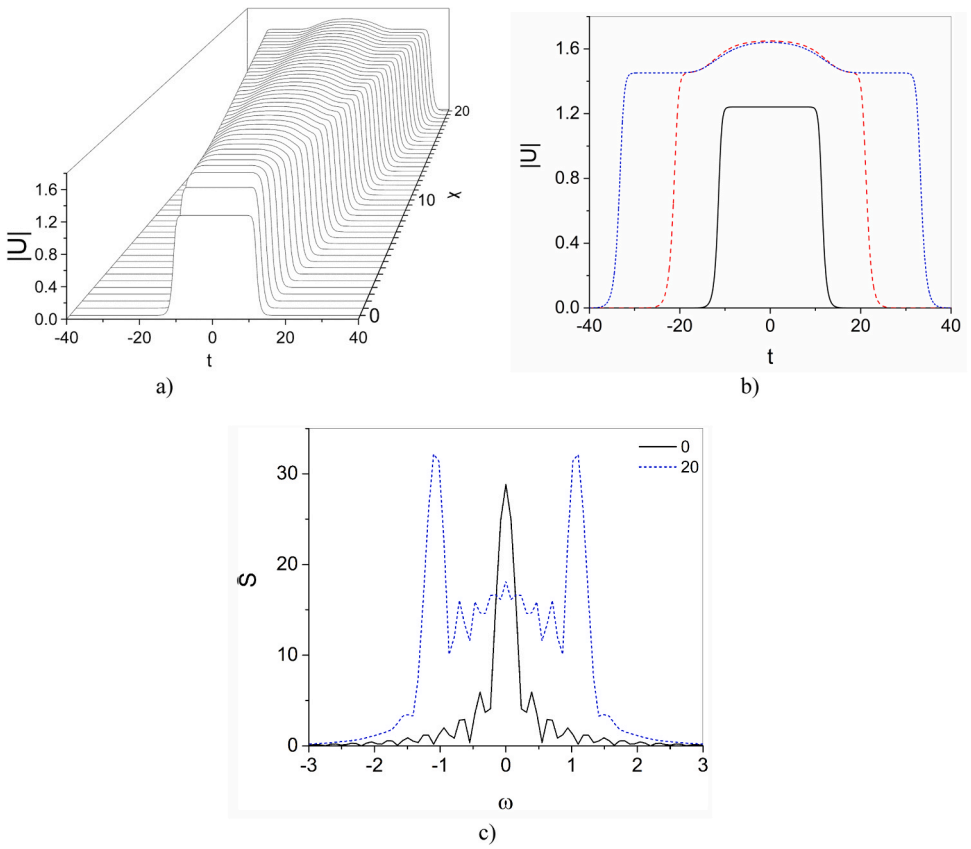

Fig. 3. Illustration of: (a) front propagation with $t_0 = 10$; (b) the amplitude at fixed distances: $x = 0$, (black solid line), 10 (red dash line) and 20 (blue short-dash line); and (c) the spectrum amplitude at fixed distances 0 (black solid line) and 20 (blue short-dash); Parameters: $\delta = -0.0145769$, $\beta = 0.28$, $\varepsilon = 0.742$, $\nu = -0.482143$, $\mu = -0.2771$,$\gamma = 0$. (For interpretation of the references to color in this figure legend, the reader is referred to the web version of this article.)

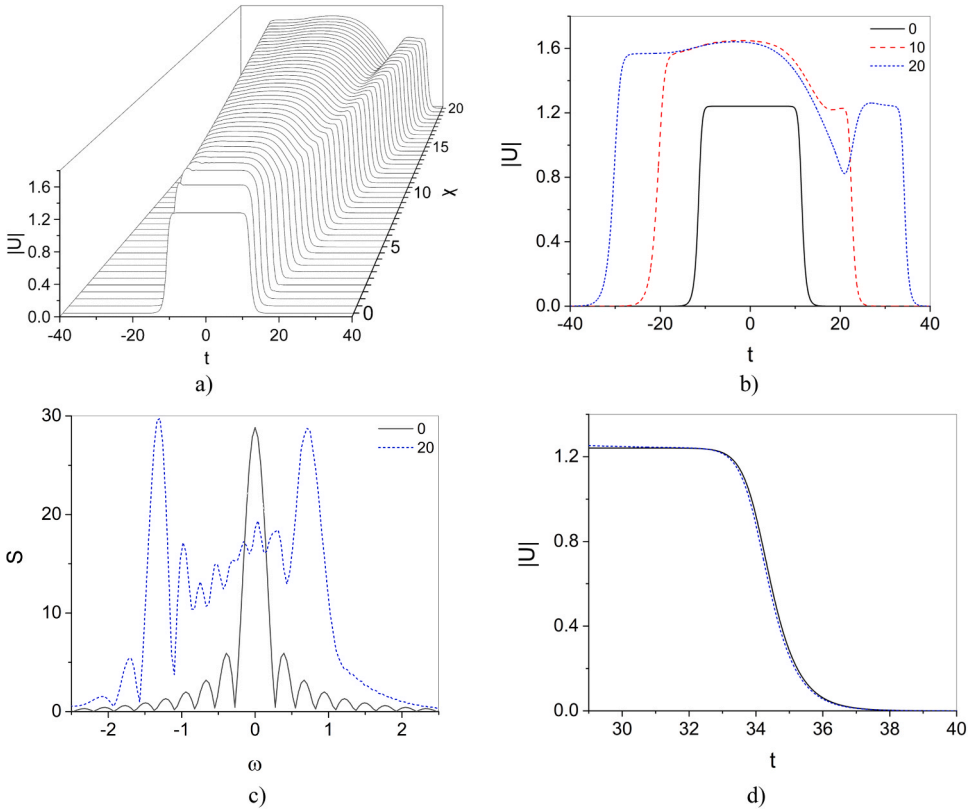

Fig. 4. (a) The front propagation with $t_0 = 10$; (b) the corresponding amplitude at fixed distances: $x = 0$, (black solid line), $x = 10$ (red dash line) and $x = 20$ (blue short-dash line); c) the spectrum amplitude at $x = 0$ (black solid line) and $x = 20$ (blue short-dash line); (d) A comparison between the exact kink solution from Eq. (21) (solid black line) time-shifted close to the numerical curve and a slice of the numerical solution taken around the right edge of the formation at $x = 20$ (blue short-dash line) is presented; Here: $\delta = -0.0145769$,$\beta = 0.28$,$\varepsilon = 0.742$,$\nu = -0.482143$,$\mu = -0.2771$ and $\gamma = 0.65$. (For interpretation of the references to color in this figure legend, the reader is referred to the web version of this article.)

each other are constant and with equal magnitude. Our numerical estimation for the velocities of left/right fronts is: 1.2048/1.2048. What we observe in Fig. 4 and Fig. 5 is that under the influence of IRS, the velocities of the kink-antikink pair are constant with distance, but now different in magnitude and larger for the kink. Numerically computed values for the velocities kink/antikink at $x = 20$ and $t_0 = 1$ are: 1.17/0.98; at $t_0 = 10$: 1.17/0.98; and at $t_0 = 20$: 1.29/1.08. Calculation of the real number M into Eq. (12) gives $M = 1.17286$. It is seen also that a very good correlation between the analytical prediction of M for $t_0 = 1$ and $t_0 = 10$, and its numerically measured values exists. Note that the velocities in the case $\gamma = 0$ exceed those with $\gamma \neq 0$.

Finally, we study the stability of the propagation of the exact solution with respect to the initial condition through the usage of a super-Gaussian pulse $U(t) = \exp[-(t/5)^4]$ as an initial input. The result is presented in Fig. 6.

Comparing the results presented in Fig. 6a, b with those in Fig. 4 we conclude that the propagation of a super-Gaussian pulse is very similar to the propagation our kink-antikink formation with the same width. This small dependence from the initial condition in the equation like CCGLE has been mentioned earlier.

5. Conclusion

The paper reports the results of a combined analytical and numerical study of the complex cubic–quintic Ginzburg-Landau equation (CCQGLE) and CCQGLE perturbed with the term responsible for the intrapulse Raman scattering (IRS). Using the approaches of Akhmediev et al. [9,15,16] and Uzunov and Georgiev [32], novel exact kink and antikink solutions of these types of complex Ginzburg-Landau equations are identified by applying the method of first-order autonomous sub-equations, see Conte and Musette [19]. The foregoing solitary wave solutions are represented in explicit analytic form. Results of a numerical study of the influence of the IRS on the front solutions of CCQGLE are presented too. Agrawal's split-step Fourier method with two iterations [44,45] was applied in our numerical analysis. We have explored the possibility to identify the novel kink solution given by Eq. (21) in the process of front propagation described by the numerical solution of CCQGLE. A good correlation between obtained numerical results for the shape, amplitude, and velocity of the right part of the front and those characteristics of the predicted novel kink solution has been established. It has also been established that such a good correlation between the right part of the propagating front and the characteristics of novel kink solutions conserves for the following different initial conditions: a) formation of kink and antikink, and b)

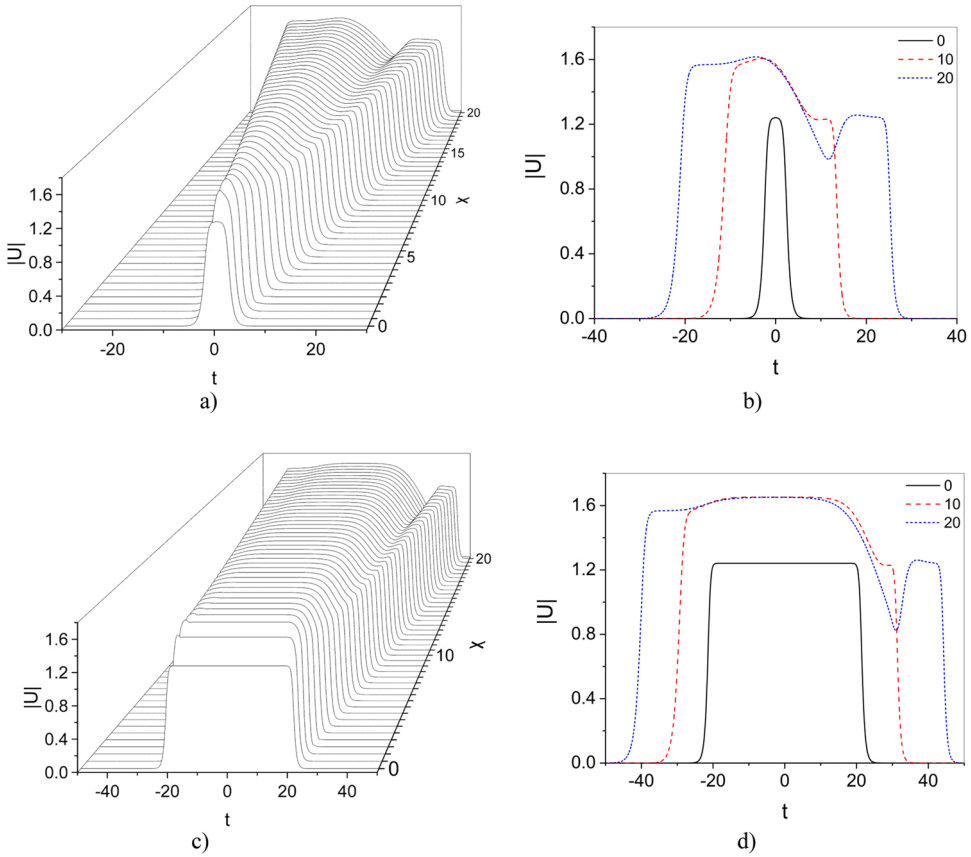

Fig. 5. The fronts propagation (a) for. and (c) $t_0 = 20$; the temporal shapes at fixed distances $x = 0$ (black solid line), $x = 10$ (red dash line) and $x = 20$ (blue short-dash line) b) for $t_0 = 1$ and d) $t_0 = 20$. Here $\delta = -0.0145769$, $\beta = 0.28$, $\varepsilon = 0.742$, $\nu = -0.482143$, $\mu = -0.2771$ and $\gamma = 0.65$. (For interpretation of the references to color in this figure legend, the reader is referred to the web version of this article.)

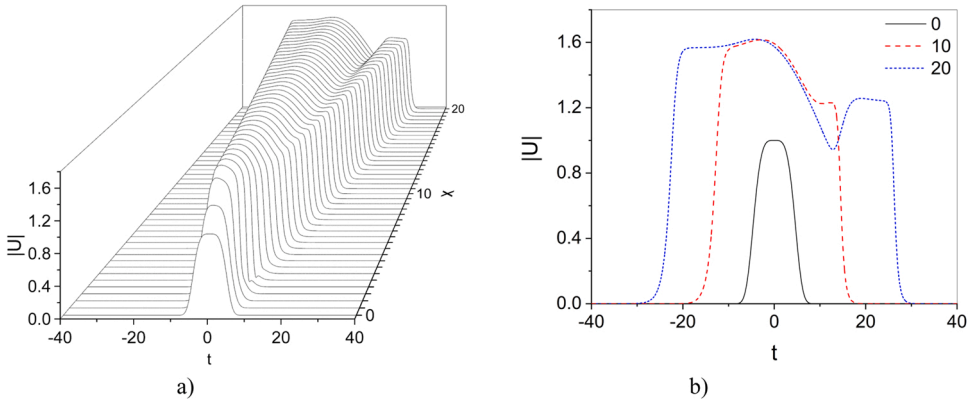

Fig. 6. Illustration of: (a) front propagation for the initial condition $U(t) = \exp[-(t/5)^4]$; b) the temporal shapes at fixed distances: $x = 0$, (black solid line), $x = 10$ (red dash line) and 20 (blue short-dash line). Here the values of the parameters are: $\delta = -0.0145769$, $\beta = 0.28$, $\varepsilon = 0.742$, $\nu = -0.482143$, $\mu = -0.2771$ and $\gamma = 0.65$. (For interpretation of the references to color in this figure legend, the reader is referred to the web version of this article.)

super-Gaussian pulses.

Declaration of Competing Interest

The authors declare that they have no known competing financial interests or personal relationships that could have appeared to influence the work reported in this paper.

Data availability

No data was used for the research described in the article.

Acknowledgements

The work of the second author V.M.Vassilev has been accomplished with the financial support by Grant No BG05M2OP001-1.002-0011-C02 financed by the Science and Education for Smart Growth Operational Program (2014–2020) and co-financed by the European Union through the European structural and Investment funds. V.M.Vassilev would like to acknowledge also the support from the Bulgarian Science Fund under grant КП-06-Н22/2.

References

[1] A. Hasegawa, F. Tappert, Transmission of stationary nonlinear optical pulses in dispersive dielectric fibers. I. Anomalous dispersion, Appl. Phys. Lett. 23 (1973) 142–144.
[2] A. Hasegawa, F. Tappert, Transmission of stationary nonlinear optical pulses in dispersive dielectric fibers. II. Normal dispersion, Appl. Phys. Lett. 23 (1973) 171–172.
[3] M. Matsumoto, H. Ikeda, T. Uda, A. Hasegawa, Stable soliton transmission in the system with nonlinear gain, J. Lightwave Technol. 13 (4) (1995) 658–665.
[4] H.A. Haus, Theory of mode locking with a fast saturable absorber, J. Appl. Phys. 46 (7) (1975) 3049–3058.
[5] H.A. Haus, J.G. Fujimoto, E.P. Ippen, Structures for additive pulse mode locking, J. Opt. Soc. Am. B 8 (1) (1991) 2068–2076.
[6] A. Hasegawa, Y. Kodama, Solitons in Optical Communications, Clarendon Press, 1995.
[7] G.P. Agrawal. Nonlinear Fiber Optics, sixth ed., Academic Press, Elsevier, 2019.
[8] G.P. Agrawal. Applications of Nonlinear Fiber Optics, third ed., Academic Press, Elsevier, 2020.
[9] N.N. Akhmediev, A. Ankiewicz, Solitons: Nonlinear Pulses and Beams, Chapman and Hall, London, 1997.
[10] N.N. Akhmediev, A. Ankiewicz, Dissipative solitons, in: N.N. Akhmediev, A. Ankiewicz (Eds.), Lecture Notes in Physics, 661, Springer, Berlin, 2005.
[11] J.N. Kutz, Mode locked soliton lasers, SIAM Rev. 48 (4) (2006) 629–678.
[12] A. Komarov, H. Leblond, F. Sanchez, Quintic complex Ginzburg Landau model for ring fiber-laser, Phys. Rev. E 72 (2005), 025604.
[13] E. Ding, P. Grelu, J.N. Kutz, Dissipative soliton resonance in a passively mode-locked fiber laser, Opt. Lett. 36 (2011) 1146–1148.
[14] W. van Saarloos, P.C. Hohenberg, Fronts, pulses, sources and sinks in generalized complex Ginzburg-Landau equations, Phys. D. 56 (1992) 303–367.
[15] N. Akhmediev, V.V. Afanasjev, Novel arbitrary-amplitude soliton solutions of the cubic-quintic complex Ginzburg-Landau equation, Phys. Rev. Lett. 75 (12) (1995) 2320–2323.
[16] N.N. Akhmediev, V.V. Afanasjev, J.M. Soto-Crespo, Singularities and special soliton solutions of the cubic-quintic complex Ginzburg-Landau equation, Phys. Rev. E 53 (1) (1996) 1190–1201.
[17] J.M. Soto-Crespo, N. Akhmediev, A. Ankiewicz, Pulsating, creeping, and erupting solitons in dissipative systems, Phys. Rev. Lett. 85 (2000) 2937–2940.
[18] N.N. Akhmediev, J.M. Soto-Crespo, G. Town, Pulsating solutions, chaotic solutions, period doubling, and pulse coexistence mode-locked lasers: complex Ginzburg-Landau equation approach, Phys. Rev. E 63 (2001), 056602.
[19] R. Conte , M. Musette, Solitary waves of nonlinear nonintegrable equations, in: N. Akhmediev, A. Ankiewicz, (Eds.), Dissipative Solitons, Volume 661 of Lecture Notes in Physics, Springer, Berlin Heidelberg, 373–406, 2005.
[20] T. Kapitula, B. Sandstete, Instability mechanism for bright solitary-wave solution to the cubic-quintic Ginzburg-Landau equation, JOSA B 15 (1998) 2757–2762.
[21] E.M. Dianov, A.Ya Karasik, P.V. Mamyshev, A.M. Prokhorov, V.N. Serkin, M.F. Stel'makh, A.A. Fomichev, Stimulated-Raman conversion of multisoliton pulses in quartz optical fibers, JETP Lett. 41 (6) (1985) 294–297.
[22] F.M. Mitschke, L.F. Mollenauer, Discovery of the soliton self-frequency shift, Opt. Lett. 11 (10) (1986) 659–661.
[23] V.N. Serkin, Colored envelope solitons in optical fibers, Sov. Tech. Phys. Lett. 13 (7) (1987) 320–321.
[24] R.H. Stolen, J.P. Gordon, W.J. Tomlinson, H.A. Haus, Raman response function of silica fibers, JOSA B 6 (1989) 1159–1166.
[25] S.C.V. Latas, M.F.S. Ferreira, M.V. Facao, Impact of higher-order effects on pulsating, erupting and creeping solitons, Appl. Phys. B 104 (1) (2011) 131–137.
[26] I.M. Uzunov, Zh.D. Georgiev, T.N. Arabadzhiev, Transitions of stationary to pulsating solutions in the complex cubic-quintic Ginzburg-Landau equation under the influence of nonlinear gain and higher-order effects, Phys. Rev. E 97 (2018), 052215.
[27] I.M. Uzunov, T.N. Arabadzhiev, S. Nikolov, Self-steepening and intrapulse Raman scattering in the presence of nonlinear gain and its saturation, Optik 271 (4) (2022), 170137.
[28] D.N. Christodoulides, Fast and slow Raman shock-wave domains in nonlinear media, Opt. Commun. 86 (1991) 431–436.
[29] G.P. Agrawal, C. Headley, Kink solitons and optical shocks in dispersive nonlinear media, Phys. Rev. A 46 (3) (1992) 1573–1577.
[30] A. Ankiewicz, N. Akhmediev, Moving fronts for complex Ginzburg-Landau equation with Raman term, Phys. Rev. E 58 (5) (1998) 6723–6727.
[31] J.M. Soto-Crespo, N. Akhmediev, Exploding soliton and front solutions of the complex cubic-quintic Ginzburg-Landau equation, Math. Comput. Simul. 69 (2005) 526–536.
[32] I.M. Uzunov, Z.D. Georgiev, Localized pulsating solutions of the generalized complex cubic-quintic Ginzburg–Landau equation, J. Comput. Methods Phys. (2014) 1–13.
[33] A.F. Sidorov, V.P. Shapeev, N.N. Ianenko, The method of differential relations and its applications in gas dynamics, Novosibirsk Izdatel'stvo Nauka (1984) (in Russian).
[34] P.J. Olver, Direct reduction and differential constraints, Proc. R. Soc. Lond. A444 (1994) 509–523.
[35] V.K. Andreev, O.V. Kaptsov, V.V. Pukhnachov, A.A. Rodionov, Applications of Group-Theoretical Methods in Hydrodynamics, Springer, Dordrecht, 1998.
[36] A.D. Polyanin, V.F. Zaitsev, A.I. Zhurov, Methods for Solving Nonlinear Equations of Mathematical Physics and Mechanics, Fizmatlit, Moscow, 2005.
[37] F.D. Tappert, Applications of fast Fourier transforms in the numerical simulation of wave propagation, Trans. Am. Nucl. Soc. 15 (1972) 277.
[38] F.D. Tappert, R.H. Hardin, Applications of the split-step Fourier method to the numerical solution of nonlinear and variable coefficient wave equations, SIAM Rev. 15 (1973) 423.
[39] R.A. Fisher, W.K. Bischel, Numerical studies of the interplay between self-phase modulation and dispersion for intense plane-wave laser pulses, J. Appl. Phys. 46 (1975) 4921–4934.

[40] C.V. Shank, R.L. Fork, R. Yen, R.H. Stolen, W.J. Tomlinson, Compression of femtosecond optical pulses, Appl. Phys. Lett. 40 (1982) 761–763.
[41] V.A. Vysloukh, V.N. Serkin, Generation of high-energy solitons of stimulated Raman radiation in fiber light guides, JETP Lett. 38 (1983) 199–202, Sov. J. Exp. Theor. Phys. Lett. 38 (1983) 199–202.
[42] W.J. Tomlinson, R.H. Stolen, A.M. Johnson, Optical wave breaking of pulses in nonlinear optical fibers, Opt. Lett. 10 (1985) 457–459.
[43] E.M. Dianov, Z.S. Nikonova, A.M. Prokhorov, V.N. Serkin, Optimal compression of multisoliton pulses in fiber-optic waveguides, Pisma V Zhurnal Tekhnischeskoi Fiziki 12 (1986) 756–760; Sov, Tech. Phys. Lett. 12 (1986) 311–313.
[44] M.J. Potasek, G.P. Agrawal, S.C. Pinault, Analytical and numerical study of pulse broadening in nonlinear dispersive optical fibers, J. Opt. Soc. Am. B 3 (1986) 205–211.
[45] I.M. Uzunov, T.N. Arabadzhiev, On the efficiency of different numerical methods for the calculation of intrapulse Raman scattering of optical solitons, Opt. Quant. Electron. 51 (2019) 283.
[46] A. Liénard, Etude des oscillations entretenues, Rev. Générale De. l′′Electr. 23 (1928) 946–954, 901-912 and.
[47] M.V. Demina, Integrability and solvability of polynomial Lienard differential systems, Stud. Appl. Math. 28 (2022) 1–63, https://doi.org/10.1111/sapm.12556.
[48] M.V. Demina, D.I. Sinelshchikov, Darboux first integrals and linearizability of quadratic–quintic Duffing–van der Pol oscillators, J. Geom. Phys. 165 (2021), 104215.